Search for the 531-day-period wobble signal in the polar motion based on EEMD

Hao Ding [1#], WenBin Shen [1, 2]*,

[1] *School of Geodesy and Geomatics, Key Laboratory of Geospace Environment and Geodesy of the Ministry of Education, Wuhan University, Wuhan 430079, China*

[2] *State Key Laboratory of Information Engineering in Surveying, Mapping and Remote Sensing, China*

* *Corresponding author*: e-mail: wbshen@sgg.whu.edu.cn

Now at Institute of Earth Sciences, Academia Sinica, Taipei

Abstract

In this study, we use a nonlinear and non-stationary time series analysis method, the ensemble empirical mode decomposition method (EEMD), to analyze the polar motion (PM) time series (EOP C04 series from 1962 to 2013) to find a 531-day-period wobble (531dW) signal. The 531dW signal has been found in the early PM seires (1962-1977) but cannot be found in the recent PM seires (1978-2013) using conventional analysis approaches. By the virtue of the demodulation feature of EEMD, the 531dW can be confirmed to be present in PM based on the differences of the amplitudes and phases between different intrinsic mode functions. Results from three sub-series divided from the EOP C04 series show that the period of the 531dW is subject to variations, in the range of 530.9d-524d, and its amplitude is also time- dependent (about 2-11 mas). Synthetic tests are carried out to explain why the 531dW can only be observed in recent 30-years PM time series after using EEMD. The 531 dW is also detected in two longest available superconducting gravimeter (SG) records, which further confirms the presence of the 531dW. The confirmation of 531dW existence

could be significant in establishing a more reasonable Earth rotation model and may effectively contribute to the prediction of the PM and its mechanism interpretation.

1 Introduction

It is recognized that the polar motion (PM) contains two dominant components: the annual wobble (AW) with a 12-month period and the Chandler wobble (CW) with a 14-month period. Some researchers have suggested that the CW is highly variable with respect to its amplitude (e.g., Carter, 1981, 1982; Höpfner, 2003; Chen et al., 2009; Chen et al, 2013a, 2013b), some have considered it having double or multiple frequencies (e.g., Chao, 1983; Pan, 2012), and some have considered its frequency being invariant (e.g., Okubo, 1982; Vicente and Wilson, 1997; Gross et al., 2003; Seitz and Schmidt, 2005). If the CW is frequency modulated as Carter (1981 and 1982) suggestted, namely the frequency is governed by the magnitude, it will creates an infinite number of sidebands, arranged symmetrically about the carrier and spaced at integer multiples of the modulating frequency (Carter, 1981). The first upper and lower sidebands could be at 1 cpy (cycles per year) and 0.69 cpy respectively when the beat frequency is 0.157 cpy (CW's frequency 0.843cpy ± k×0.157; k=1 denotes the first upper and lower sidebands), where the beat frequency or beat period is the time period required for the Earth's pole to complete a cycle of the combined AW (12 months) and CW (14-months). Because the first upper sideband of the CW was contaminated in the spectrum of the AW, it was concluded that only the first lower sideband, which is located at 0.686 cpy, could most likely be detected. Based on a 16-year time series of International Polar Motion Data (spanning from 1962 to 1977), a 0.686 cpy component with its amplitude being around 10 to 17 mas (milliarcsecond) was very weakly detected in Catrer (1982), but its signal-to-noise ratio (SNR) is very low. Based on

45 the PM series (spanning from 1974 to 1981) obtained by the Doppler satellite tracking and lunar
46 laser ranging, Morgan et al. (1982) identified two spectral peaks at 532±10.8 days and 537±15.2
47 days, with their amplitudes around 8.6±2.0 mas and 7.4±2.2 mas, respectively. However, after then
48 (1980s), this signal was seldom announced in the PM time series with higher SNR (especially for the
49 records after the mid-1990s). Recently, Na et al. (2011) found a 500-day period component in the
50 PM data with an average amplitude of 20 mas, and argued that if assuming the existence of this
51 component, the RMS error of the prediction of the PM could be reduced by 50%; and suggested that
52 this phenomenon should be caused by resonance of unidentified oscillating mode of the Earth
53 (possibly Earth's inner core wobble). In addition, this wobble (or referred to as an 18-month wobble)
54 was found in the analysis of the atmospheric angular momentum data by Wahr (1983) and Chen et al.
55 (2010). Furthermore, a signal with a period about 1.5 year could be also found from the variation of
56 length of day (LOD) by using the wavelet analysis as suggested by Chao et al. (2014). To check our
57 results (this paper), King (2015) used a Kalman Filter-Smoother to analyse the PM series in the time
58 domain, and his results show that the amplitude and especially the phase of the 531dW are time vary
59 (www.nonlin-processes-geophys-discuss.net/2/C163/2015/) ; while relevant earlier results using a
60 Kalman Filter to the PM series can be found in King and Watson (2014). Besides these, in our
61 knowledge, this component was poorly studied. Inasmuch as the detection of this component could
62 be significant in establishing a more reasonable Earth rotation model and may effectively contribute
63 to the prediction of the PM, the main purpose of this study is to detect the ~530-day-period wobble
64 (simply 531dW hereafter for convenience, the reason of which could be found in section 3)
65 component and provide a possible explanation why in general cases it could not be detected from
66 observation series (e.g. EOP C04 series) based on the Fourier anaylsis.

Generally, the traditional Fourier analysis method cannot observe this 531dW signal (see Figures 2d-f), hence, in this study a nonlinear and non-stationary time series analysis method, the ensemble empirical mode decomposition (EEMD) (Huang and Wu 2008; Wu and Huang 2009) is applied to a PM time series as a filter bank to detect the 531dW signal. (To know the differences and relations between different spectral anaylsis method, we suggest the readers to refer some other literatures, such as Tary et al. (2014)) .

Here, the PM time series, the EOP C04 series spanning from 1962 to 2013 with one-day sampling interval from the International Earth Rotation and Reference System Service (IERS) (http://www.iers.org/IERS/EN/DataProducts/EarthOrientationData/), is used for observing the signal of interest.

2 Method

EEMD was proposed to overcome the disadvantages existing in the empirical mode decomposition (EMD) (Huang et al., 1998; Huang and Wu, 2008), such as the mode-mixing problem and the end effect (see as Fig. 2 in Shen and Ding (2014)), although EMD has demonstrated its applicability in a wide range of geoscience studies over the last 15 years (e.g., Pee and McMahon, 2006; Thomas et al., 2009; Franzke, 2009; Jackson and Mound, 2010; Jeng and Chen, 2011; Lee et al., 2011; Shen and Ding, 2014; Chambers, 2015). The details of EMD and EEMD can be found in many relevant literatures (e.g., Huang et al., 1998; Huang and Wu, 2008; Wu and Huang, 2009; Shen and Ding, 2014).

A given time series $x(t)$ can be decomposed into a number of intrinsic mode functions (IMFs) using the following steps (Huang and Wu, 2008; Shen and Ding, 2014):

1. Identify all local maxima and local minima of $x(t)$, where its upper (lower) envelope can be formed using a cubic spline line to connect all the local maxima (minima).

2. Use $h_1(t)=x(t) - m_1(t)$ to get a new series, where $m_1(t)$ is the mean of the upper and lower envelopes of $x(t)$. Steps 1 and 2 are called a sifting procedure.

3. Generally, $h_1(t)$ is not an IMF, hence, treat $h_1(t)$ as the data given just as $x(t)$, and repeat the sifting procedure (step 1 and 2) k times until $h_k(t)$ is an IMF, namely, $h_{1k}(t)= h_{1(k-1)}(t) - m_{1k}(t)$. Let $c_1(t)= h_{1k}(t)$, which is designated as the first IMF.

4. Then, setting $r_1(t)=x(t) -c_1(t)$, and repeating the steps 1-3 for $r_1(t)$, one can get the second IMF, $c_2(t)$.

5. Repeat the above steps, and then the j-th target IMF, $c_j(t)$, can be obtained.

The above process is the EMD. In these steps, two different iterative loops exist. The first loop is employed to obtain $h_k(t)$, in which an IMF must have a specific definition to stop circulating steps 1 and 2. In the second loop, the repeat times j must be a finite number, in which a criterion must be determined to stop the entire sifting process. For the first loop, Huang *et al*. (1998) limited the size of the standard deviation, $SD_k = \sum_{t=0}^{T} |m_{1k}|^2 \Big/ \sum_{t=0}^{T} |h_{1k}|^2$, which was computed from the two consecutive sifting results to stop this loop. SD_k can be generally set between 0.2 to 0.3. The second loop can be terminated by either of the two criteria: (1) the component c_n or the residue r_n becomes so small that it is less than the previously given value of the substantial consequence; or (2) no more IMF can be extracted from r_n (see also in Shen and Ding, 2014).

Given that EMD has the mode-mixing problem and end effects, EEMD is developed with the following procedures (Huang and Wu, 2008; Shen and Ding, 2014):

1. Add a white noise series to the targeted time series $x(t)$;

2. Decompose the series with added white noise into IMFs;

3. Repeat procedures 1 and 2 iteratively, but with different white noise series each time;

4. Obtain the (ensemble) means of the corresponding IMFs of the decompositions as the final IMF.

In the decomposition using EEMD, the added white noise series cancel each other in the final mean of the corresponding IMF. Note that in the EEMD process, the procedure 2 is just the whole EMD process. The means of the IMFs remain within the natural filter windows, significantly reducing the possible of mode mixing and preserving the filter property (Huang and Wu, 2008; Shen and Ding, 2014).

By using EEMD, the chosen time series can be decomposed into a finite number of simple IMFs, and different-scales signals in the series will be re-combined by proper IMFs based on the fact that different IMFs have different frequency bands. Hence, for the chosen EOP C04 series, $f(t)$, and its IMFs satisfy the following linear equation

$$f(t) = \mathrm{IMF1}(t) + \mathrm{IMF2}(t) + \ldots + \mathrm{IMF}n(t) + r(t). \quad (1)$$

where n is the number of the IMFs and $r(t)$ is a residue term. In addition, EEMD can be used to demodulate a frequency-modulated time series (Huang et al., 1998; Huang and Wu, 2008). That means EEMD can be used not only as a filter bank but also as a demodulator simultaneously. Since EEMD has these two advantages, we use it to detect the 531dW in the PM.

A frequency modulation signal can be expressed as follows (Cater, 1981 and 1982),

$$e_t(x,y) = C_c \sin[\phi_0 + 2\pi f_c t + M \cdot \sin(2\pi f_m t)]. \quad (2)$$

where $e_t(x,y)$ is the expected value of the x-component or y-component, f_m the frequency of the modulating signal, here we set it to be equal to 0.157 cpy (the beat frequency between the CW and

AW); f_c and C_c are the frequency and amplitude of the CW, and M is the modulation index, defined as $M=\Delta f/f_m$, where Δf is the maximum variation of f_m; ϕ_0 is the initial phase, and it is simply set as zero (same as the AW and the 531dW).

3 Results

3.1 Results from the PM series with/without using EEMD

The waveforms of the two compponents, the x- and y- components of the chosen PM series are shown in Fig. 1(a), and their corresponding Fourier spectra are shown in Figs. 1(b,c) (see the black bold curves, we call them the original spectra). The vertical dashed lines (Fig.1b and 1c) locate at the target freuquency, 0.6875cpy, and there is no peak that can be identified for the 531dW based on the original PM series. Meanwhile, if the EEMD is used on these two components, 11 IMFs can be obtained, respectively (see Fig. 2 for the waveforms of the IMFs of the x-component). In the Fourier spectra of IMF5 and IMF6, the 531dW can be clearly detetcted (see the blue and red curevs in Figs. 1b and 1c). The spectra for other IMFs (sum) of x- and y-components are denoted by the green curves (we call them the residual spectra). No peak can be identified for the 531dW in the residual spectra. The amplitudes of the 531dW signals in IMF5 and IMF6 are denoted by the green and red arrows respectively. Comparing with the original spectra, the amplitudes in IMF5 and IMF6 are outstanding (Figs. 1b and 1c); the phases of the IMF5 and IMF6 are almost opposite (Figs. 1d and 1e; it might be caused by the demodulation feature of EEMD). According to Equation (1), the mean amplitudes of 531dW in x- and y- components achieve 7.1 and 7.2 mas, respectively; while the corresponding noise level is about 4mas. The low SNR might be the reason why we cannot identify the 531dW signal directly from the original PM time series spanning from 1962 to 2013. However,

previous studies show that this signal has been found in the 1962-1977 PM series (see Carter 1981, 1982). One possible inference is that the amplitude of the 531dW may be varing with time. Hence, we divide the 1962-2013 PM series into three sub-series, 1962-1977 series, 1978-1994 series and 1995-2013 series, to further study the 531dW signal. Note that after 1980, the EOP time series is generated from the modern geodetic observations, and the precision of the time series has been highly improved. However, given that the EEMD is actually based on the waveform of the time series to filter different signals for different IMFs, we have confirmed that the distinction at 1980 will not significantly affect our results.

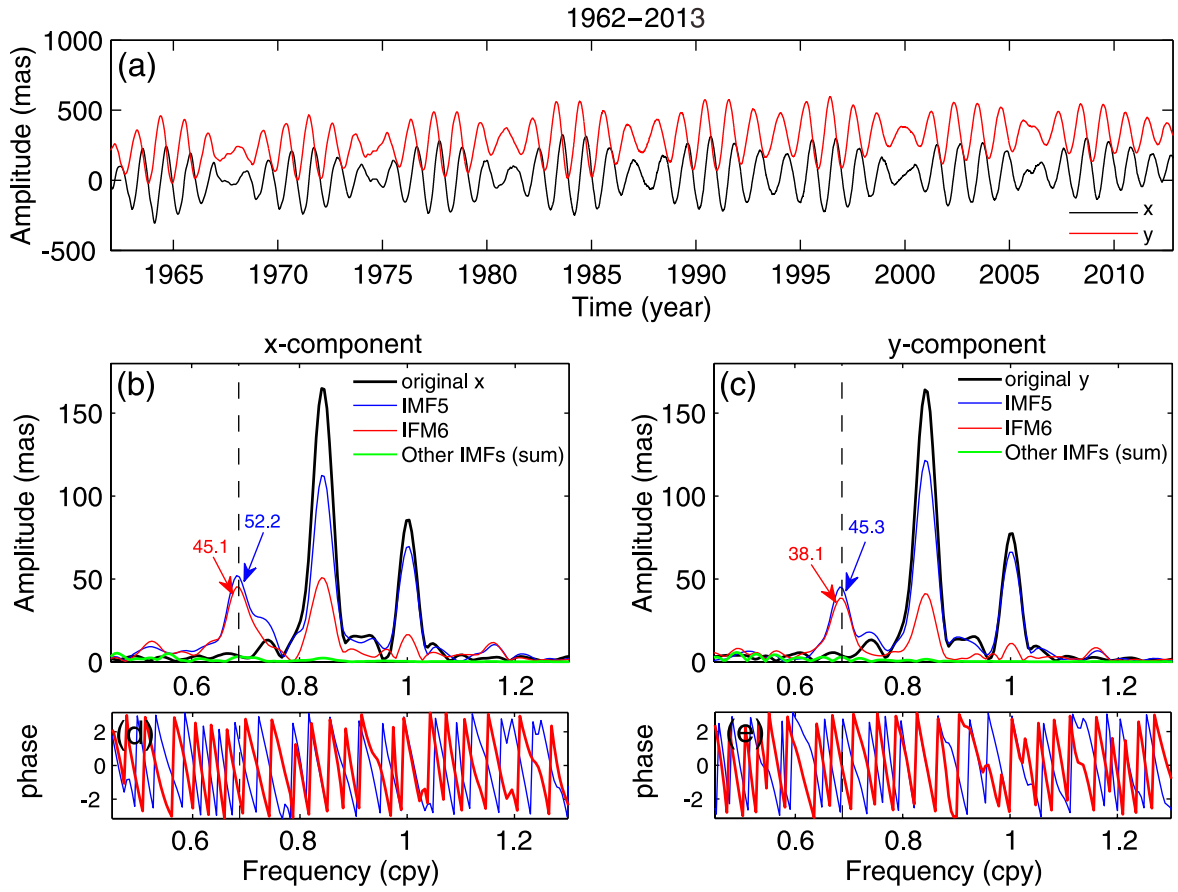

Figure 1. The x- (black) and y-components (red) of the 1962-2013PM series (a) and their corresponding Fourier amplitude spectra (original spectra, denoted by the black curves in b and c). (b)

167 x-component; (c) y-component. The spectra for IMF5 and IMF6 after applying EEMD to x- and y-
168 conponments are indicated by blue and red curevs; and their corresponding phases (based on
169 Discrete Fourier Transform) are shown in (d) and (e), respectively. The spectra (residual spectra) for
170 other IMFs (sum) of x- and y-components are denoted by the green curves.
171

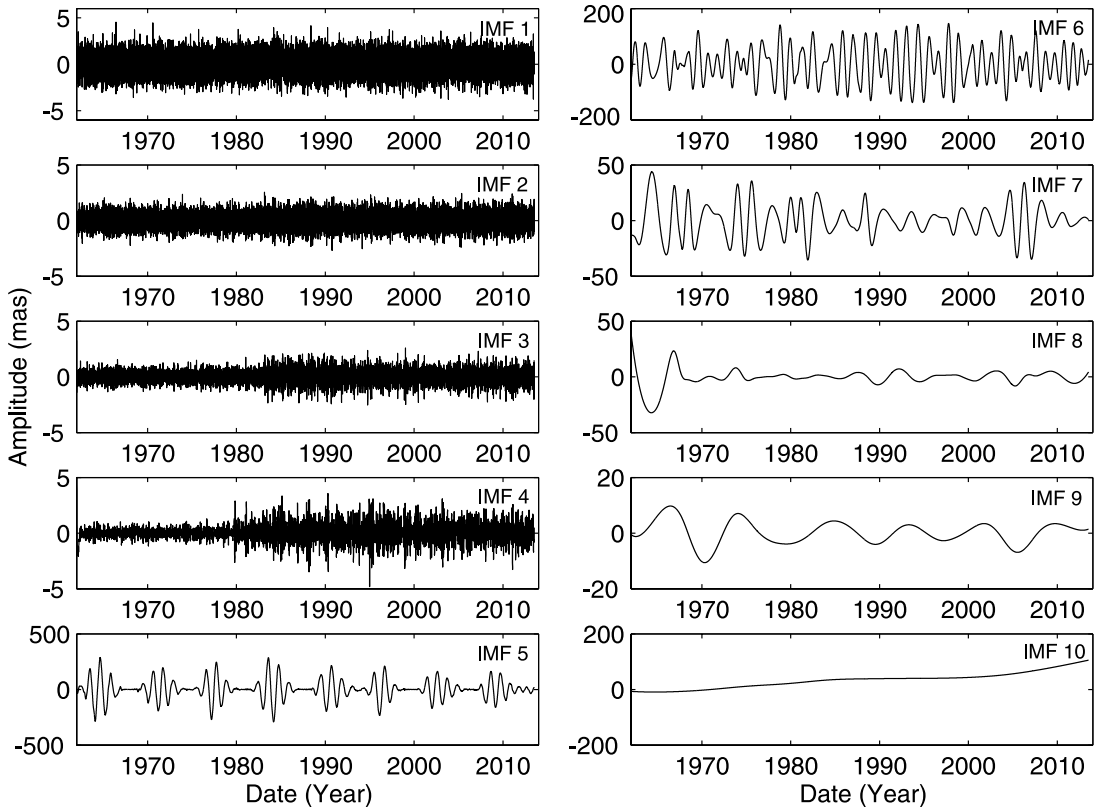

172

173 **Figure 2**. The first 10 IMFs of the x-component of the 1962-2013 PM time series after using EEMD.
174 The last one, IMF11, a linear term, is here ignored.
175

176 Based on the conventional Fourier anaylsis approach, the results as shown in Fig. 3 clearly
177 indicate that only the target peak in the spectra of the 1962-1977 series (see Fig. 3b) is over their
178 corresponding background noise level (see Fig. 3d; note that a 0.57 cpy peak in Fig. 3f is also over
179 the noise level, but it is not the interesting signal of this study), which is consistent with previous

studies (Carter, 1981 and 1982; Morgan et al., 1982). Without using EEMD, our estimates for the target 531dW, CW, and AW (the annual wobble) are tabulated in Table 1 (Note that the estimations for the amplitudes, frequencis and their corresponding error bars are obtained by using the AR method proposed by Chao and Gilbert (1980), more details can be found in Ding and Shen (2013), and Ding and Chao (2015)). For the *x*- and *y*-components of the 531dW signal from the 1962-1977 series, the corresponding amplitudes are 11.3 mas and 14.6 mas, while the estimates of previous studies are about 8 mas (Carter, 1981 and 1982; Morgan et al., 1982). However, this wobble cannot be found in the 1978-1994 and 1995-2013 series.

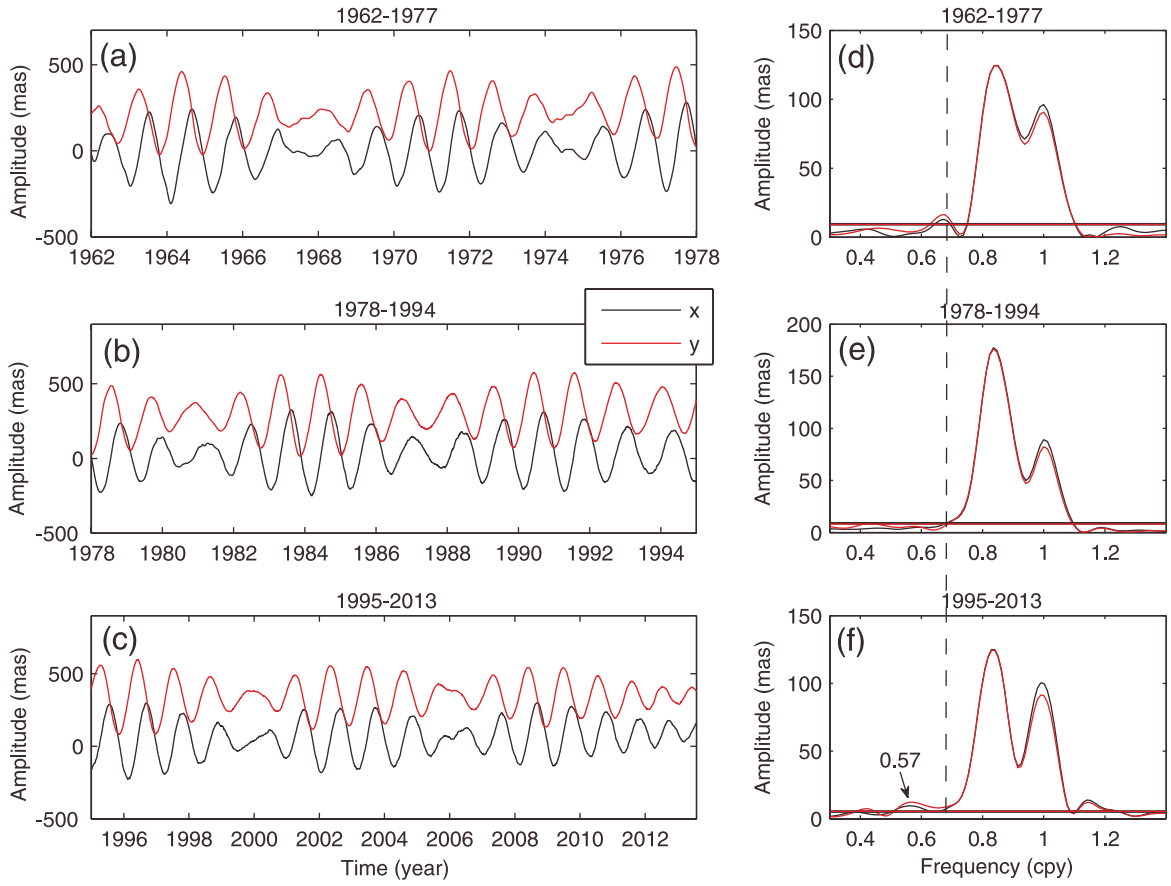

Figure 3. The three sub-series divided from the EOP C04 series (1962-2013) and their

corresponding amplitude spectra. The vertical dashed line locates at the 0.687 cpy, and the horizontal lines denote the RMS noise amplitudes of the frequency bands 0.2-0.75 cpy and 1.05-2.0 cpy, which are used as the background noise levels of their corresponding spectra. For the *x*- and *y*-components of the 1962-1977 series, the RMS noise amplitudes are 9.5 mas and 9.2 mas, respectively; for those of the 1978-1994 series, they are 8.8 mas and 8.2 mas; for those of the 1995-2013 series, they are 5.4 mas and 5.5 mas.

Table 1. The observed frequencies (cpy) and amplitudes (mas) of the CW, AW and the target wobble. The estimations are obtained by the AR method (Chao and Gilbert, 1980).

		Target Wobble		Chandler Wobble		Annual Wobble	
		Frequency	Amplitude	Frequency	Amplitude	Frequency	Amplitude
1962-1977	*x*-Component*	0.68751±6.6e-4	11.3±5.2	0.84381±5.8e-4	129.2±7.2	1.00023±6.2e-4	97.1±8.9
	x-IMF5	0.68749±7.0e-4	44.1±7.4	0.84380±6.2e-4	103.6±7.4	1.00019±7.3e-4	73.1±9.2
	x-IMF6	0.68750±7.2e-4	33.2±8.5	0.84381±1.1e-3	25.1±9.9	1.00021±1.2e-3	24.6±10.4
	y-Component*	0.68753±6.8e-4	14.6±5.5	0.84383±6.3e-4	129.2±7.0	1.00028±6.5e-4	90.8±8.5
	y-IMF5	0.68752±7.1e-4	44.9±7.7	0.84384±6.8e-4	104.0±7.3	1.00027±7.9e-4	73.2±8.7
	y-IMF6	0.68753±8.0e-4	32.7±9.2	0.84384±1.7e-3	23.8±10.5	1.00031±1.9e-4	18.5±10.9
1978-1994	*x*-Component*	--	--	0.84312±4.1e-4	180.1±4.4	1.00031±5.4e-4	90.6±6.3
	x-IMF5	0.69614±6.8e-4	50.0±6.7	0.84311±5.2e-4	145.5±5.3	1.00027±6.3e-4	83.9±6.1
	x-IMF6	0.69611±7.4e-4	45.3±8.1	0.84309±8.6e-4	27.2±8.3	--	--
	y-Component*	--	--	0.84314±4.2e-4	180.1±4.2	1.00029±5.8e-4	84.1±6.5
	y-IMF5	0.69617±7.3e-4	50.5±6.5	0.84316±5.0e-4	153.3±5.0	1.00028±6.6e-4	82.0±7.0
	y-IMF6	0.69613±7.9e-4	44.1±6.8	0.84314±7.9e-4	29.9±7.9	--	--
1995-2013	*x*-Component*	--	--	0.83892±1.9e-4	128.0±2.1	1.00030±2.8e-4	100.8±3.6
	x-IMF5	0.68644±4.2e-4	31.2±6.1	0.83895±2.6e-4	81.1±3.4	1.00025±3.7e-4	63.0±4.4
	x-IMF6	0.68646±6.3e-4	33.3±5.9	0.83893±5.3e-4	46.6±4.1	1.00031±6.3e-4	39.2±5.6
	y-Component*	--	--	0.83893±1.8e-4	128.2±1.9	1.00027±3.0e-4	91.8±4.0
	y-IMF5	0.68648±4.1e-4	32.8±5.7	0.83897±2.4e-4	86.6±3.0	1.00027±3.5e-4	63.6±4.3
	y-IMF6	0.68644±5.7e-4	33.3±5.5	0.83894±4.3e-4	37.9±3.8	1.00031±6.3e-4	28.5±5.5

* Directly estimated values from observation series without using EEMD.

Table 2. The vector differences of the amplitudes of IMF 5 and IMF6 for the three sub-series

(frequency domian). (unit: mas)

		1962-1977	1978-1994	1995-2013
x-component	531dW	12.8	4.0	3.4
	RMS noise level	9.5	8.8	5.4
y-component	531dW	16.4	8.7	3.9
	RMS noise level	9.2	8.2	5.5

After apppling EEMD to the three sub-series, only IMF5 and IMF6 contain the 531dW signal, the corresponding spectra being shown in Fig. 4 (for x-component) and Fig. 5 (for y-component). As for other IMFs, the corresponding peaks at 531dW frequency can neither exceed the background noise levels of their spectra just as in the whole 1962-2013 PM series they cannot (see the green curves in Fig. 1). Note that we do not rule out the possibility that some part (energy) of the interesting signals may also present in the adjacent IMFs, but they must be very weak (see Fig. 1) so that they can be neglected. Hence, in the present case, we will only concern the IMF5 and IMF6.

As shown in Figs 4 and 5, the phases for CW (and AW) in IMF5 and IMF6 are same (except for IMF 6 in Figs 4c and 5c, where there is no peak for AW), whereas the phases for the 531dW in IMF5 and IMF6 are quite different. The corresponding amplitude and frequency estimates are listed in Table 1. Taking into account the same phases as shown in Figs 4 and 5, one can find that the amplitudes from the IMFs for CW and AW are consistent with the results without using EEMD (see Table 1). As for the amplitudes of the 531dW in three sub-series, we use the vector difference to estimate the relevant values. The corresponding results are shown in Table 2. Considering the estimation errors, Table 2 also indicates that the 531dW cannot be found in the spectra by using the Fourier analysis (as shown in Figs 3e and 3f).

Wahr (1983) implied that there exists a 18-month (~547day) polar wobble (which can be

222 considered as coinciding with the 531dW signal mentioned in the present paper), which could be
223 caused by oceanic excitation. Chen et al. (2010) further demonstrated that the atmospheric excitation
224 may give rise to the 531dW signal with an amplitude 15 mas using the atmospheric angular
225 momentum (AAM) dataset spanning from 1948 to 2006. But from the above results, those excited
226 531dW signals almost disappear from the 1978-1994, and 1995-2013 series. This might be due to the
227 fact that the 531dW signal has varying amplitudes and phases with time. However, after using
228 EEMD, the 531dW signals can be detected in two IMFs with very different phases. Hence, we may
229 carefully suggest that this phenomenon can be explained by the demodulation feature of EEMD. And
230 this feature of EEMD gives us a chance to confirm that the 531dW is present in PM due to the
231 differences of the phases between different IMFs.
232
233

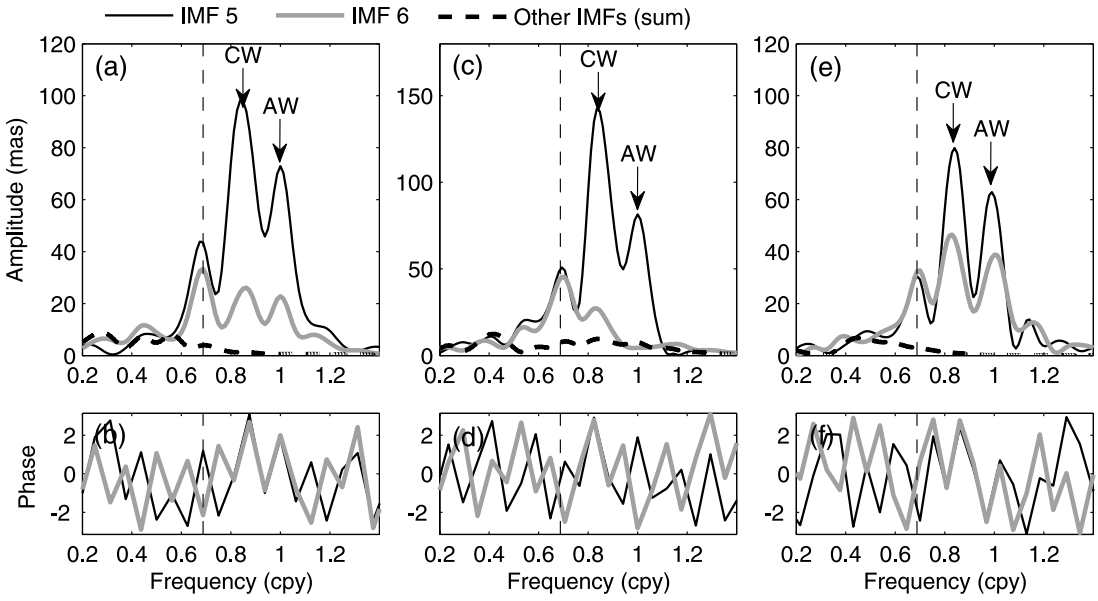

234
235 **Figure 4**. The amplitudes and phase spectra of the IMF 5, IMF 6 and the sum of the other IMFs of
236 the *x*-components of the three sub-series after using EEMD. a)-b), c)-d) and e)-f) for the 1962-1977,
237 1978-1994 and 1995-2013 series, respectively. The vertical dashed lines denote the possible spectral

peaks for the 531dW.

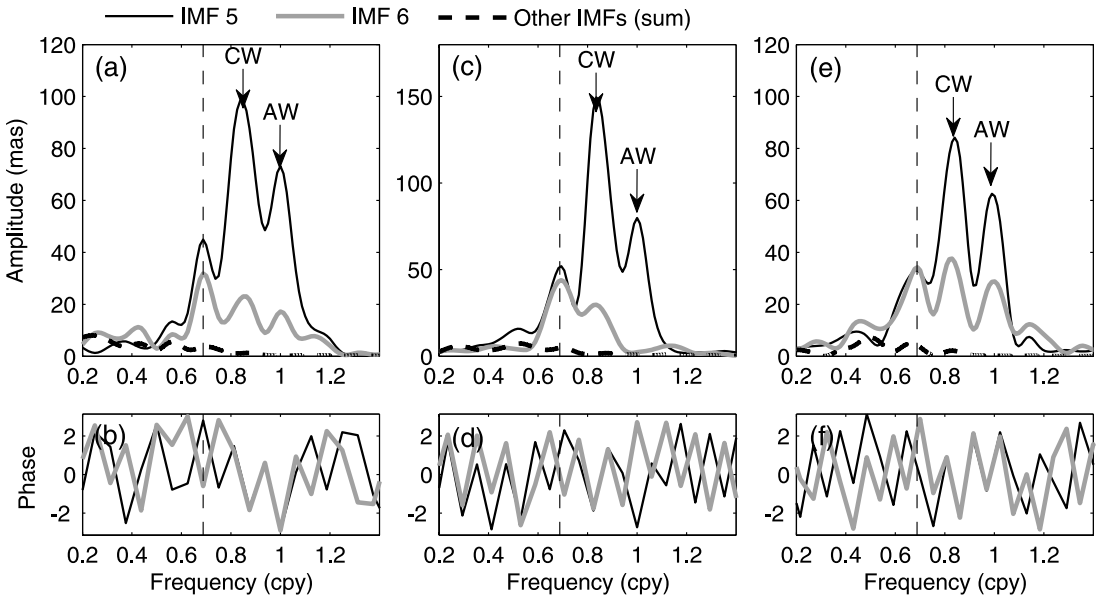

Figure 5. Same as Figure 4, but for the *y*-components of the three sub-series.

3.2 Synthetic tests for the frequency modulation and demolulation

By carefully examining Table 1 we can find that the amplitudes of the 531dW in IMF6 perhaps have some proportional relation with the amplitudes of CW in their corresponding x-/y-components without using EEMD (namely those two corresponding amplitudes for x- (or y-) component have almost linear relationship (considering the error bar), see Table 1), whereas the amplitudes of the 531dW in IMF5 and their corresponding CW amplitudes in x-/y-components without using EEMD have no obvious linear relationship. According to previous studies, here we assume that the amplitude of the 531dW in IMF6 is caused by the frequency modulation of CW.

The expression of the frequency modulation signal can be found in Eqution (2) in the Section 2. From Table 1, we can get the amplitudes of the *x*- and *y*- components of the three sub-series (without using EEMD), hence, we use those parameters to generate three synthetic noise-free time series

254 based on Equation (2), and they have the same sampling intervals and lengths as the 1962-1977,
255 1978-1994, and 1995-2013 series, respectively. As previous studies suggested (Carter, 1981 and
256 1982), we first test the modulation index *M* of CW which equals 0.23 and 0.38 respectively, and set
257 different amplitudes for the CW and AW to ensure that the synthetic spectra coincide with the
258 spectra of the actual observations (here we use the *x*-components of the three sub-series as examples),
259 and the frequencies of the CW and AW are set to 0.8437 and 1.00 cpy. The set amplitude parameters
260 (input) and their corresponding synthetic output are listed in Table 3. The corresponding spectral
261 results are shown in Fig. 6. From Table 1 and Fig. 6, one can clearly find that if *M*=0.23, for the
262 1962-1977 series, the amplitude (x-component) of the sideband that is caused by the frequency
263 modulation of the CW is 15.17 mas, and our estimates from the 1962-1977 series are about 11.3 and
264 14.6 mas for *x*- and *y*-components, respectively. Obviously, our synthetic result is consistent with our
265 observed results. If we only consider this fact, we may conclude that the observed target wobble
266 from the 1962-1977 series very likely originates from the frequency modulation of CW. But here we
267 do not want to infer whether the CW is frequency modulated, but obviously, the synthetic results for
268 the 1978-1994 and 1995-2013 series based respectively on *M*=0.23 and 0.38 clearly show the
269 appearance of the target wobble, whereas there is no significant peak for the target wobble in the
270 corresponding actually observed spectra. Namely, the modulation index *M*=0.23 or 0.38 of CW
271 cannot explain the observed results from the later two sub-series. Although we cannot ensure that *M*
272 is a constant, we try to find an *M* that can produce sufficient modulation for all the three sub-series.
273 We find that *M*=0.5 is a good choice.

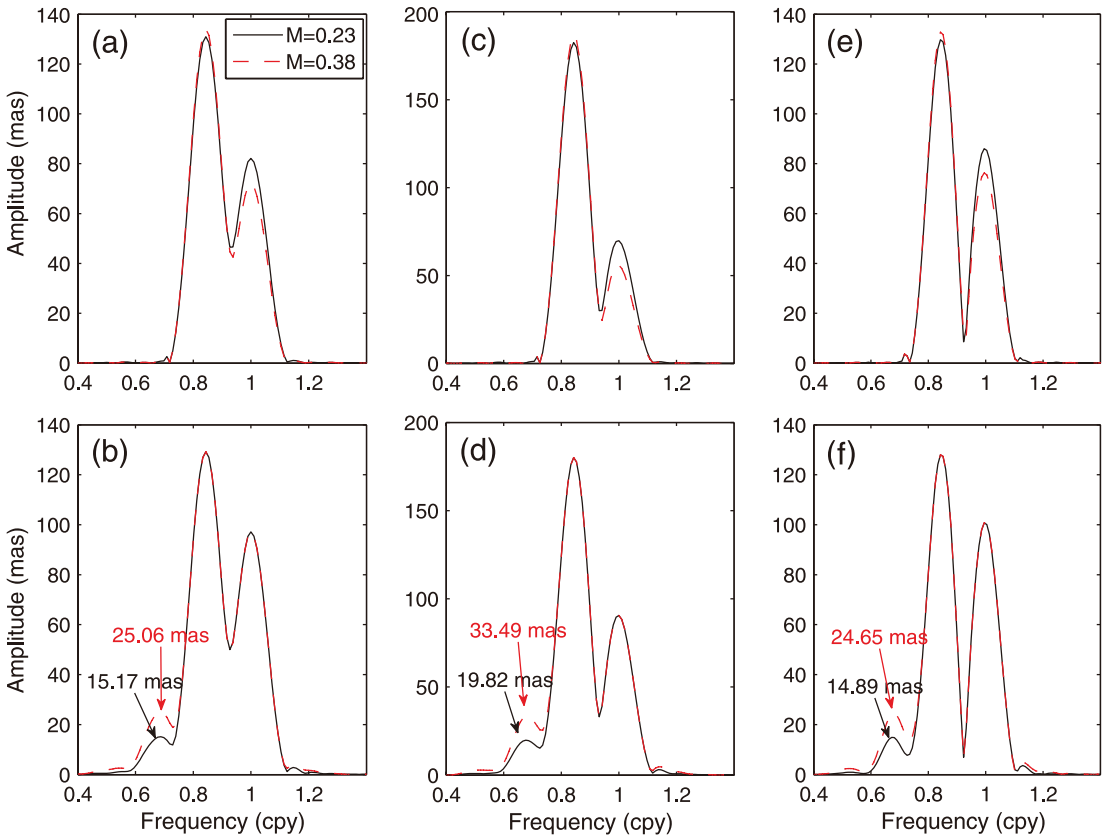

Figure 6. The amplitude spectra of the synthetic records (noise-free) based on conventional approach. a) and b), c) and d), and e) and f) for the *x*-component of the 1962-1977 series, 1978-1994 series, and 1995-2013 series, respectively. The three top figures show the results without considering the frequency modulation of CW, whereas the three bottom figures are the corresponding results with considering the frequency modulation of CW, with the modulation index M= 0.23 (black curves) and 0.38 (red dashed curves).

Now we set M=0.5, and construct three synthetic noise-free time series based on Equation 2 for the 1962-1977, 1978-1994, and 1995-2013 series, and still set different amplitudes for the CW and AW to guarantee that the theoretical spectra coincide with the observational spectra (the input parameters are the same as the parameters for the three series without considering frequency modulation of CW, which are listed in Table 4; note here only CW and AW are considered). The

corresponding results are shown in Fig. 7 (using the *x*-components as examples), and the amplitudes of the first sidebands caused by the frequency modulation of CW are marked by the arrows. The synthesis results (x components) show that the amplitudes of the 531dW in the three sub-series are respectively 33.36, 44.98, and 32.98 mas, while the corresponding results of x- and y components in IMF 6 are 33.2 (for *x*-) and 32.7 mas (for *y*-), 45.3 (for *x*-) and 44.1 mas (for *y*-), 33.3 mas (for *x*- or *y*-). Clearly, when M=0.5, the results from the frequency modulation of CW are consistent with the corresponding results in IMF6. If the 531dW in IMF6 is really caused by the frequency modulation of CW with a modulation index M=0.5, the 531dW in IMF5 may be excited by some geophysical processes, such as the atmospheric/oceanic excitation (Wahr, 1983; Chen et al., 2010), then we can appropriately explain the observations after using EEMD and the disappearance of the 531dW in the recent PM series. Here, we would like to further demonstrate that EEMD can directly demodulate a frequency-modulated time series.

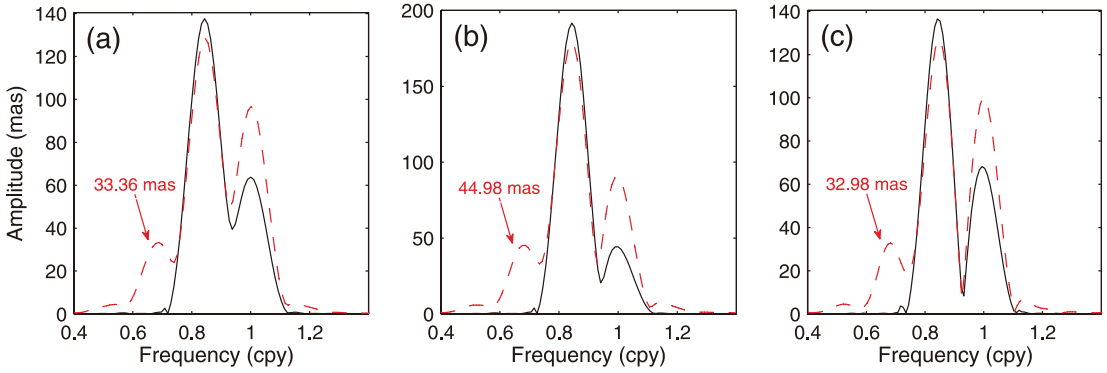

Figure 7. The amplitude spectra of the synthetic series without using EEMD. (a), (b), and (c) for the *x*-component of the 1962-1977, 1978-1994, and 1995-2013 series, respectively. The black curves indicate the results without considering the frequency modulation of CW, whereas the red dashed curves are the corresponding results when considering the frequency modulation of CW, with the

modulation index M =0.5.

Table 3. The chosen amplitudes of the CW (0.8437 cpy) and AW (1 cpy) for the synthetic series, and the corresponding estimated values from the synthetic series. (Unit: mas)

M		Synthetic (input)		Synthetic (output)		
		CW	AW	CW	AW	531dW
0.23	1962-1977	130.9	82.06	129.2	97.1	15.17
	1978-1995	181.9	68.25	180.1	90.6	19.82
	1995-2013	129.5	85.4	128.0	100.8	14.89
0.38	1962-1977	133.9	72.03	129.2	97.1	25.06
	1978-1995	186.3	54.23	180.1	90.6	33.49
	1995-2013	132.6	75.6	128.0	100.8	24.65

Table 4. The input parameters for the six synthetic series. (FM: frequency modulation)

		Synthetic series					
		I	II (FM)	III	IV (FM)	V	VI (FM)
CW	Frequency (cpy)	0.8437	0.8437	0.8437	0.8437	0.8437	0.8437
	Amplitude (mas)	137.6	137.6	191.3	191.3	136.4	136.4
AW	Frequency (cpy)	1.0000	1.0000	1.0000	1.0000	1.0000	1.0000
	Amplitude (mas)	63.7	63.7	42.6	42.6	67.4	67.4
531dW	Frequency (cpy)	0.6875	0.6875	0.6875	0.6875	0.6875	0.6875
	Amplitude (mas)	44.1	44.1	50.0	50.0	31.2	31.2

We generate six synthetic noise-free time series. The length of the synthetic series I and II is equal to that of the 1962-1977 series, the length of the synthetic series III and IV is equal to that of the 1978-1994 series, and the length of the synthetic series V and VI is equal to that of the 1995-2013 series, with one-day sampling interval. The synthetic series I (III/V) contains three sinusoidal components without frequency modulation, and the frequencies and amplitudes of CW and AW (see Table 4) are set to make the results for CW and AW after tuning the frequency modulation of CW to be the same as with the observations from the x-component of the 1962-1977

319 series (1978-1994 and 1995-2013; see Table 1 and Figs. 8b-f). The third signal is the 531dW which
320 is listed in Table 3. As for the synthetic series II (IV/VI), its parameters are the same as the synthetic
321 series I (III/V), but a mechanism of frequency modulation of CW is considered with the modulation
322 index M=0.5. The spectra of the six synthetic series are shown in Fig. 8. Obviously, after considering
323 the frequency modulation of CW, the amplitude of the 531dW in the synthetic series II is reduced to
324 only 11.05 mas, which is almost equal to the observed result obtained from the x-component of the
325 1962-1977 series without using EEMD (11.3 mas, see Fig. 3 and Table 1). The corresponding
326 spectra of the IMF5 and IMF6 of the synthetic series II obtained after using EEMD are shown in Figs.
327 8b1 and 8b3. Similar to the real data, the phases for CW (or AW) in IMF5 and IMF6 are same,
328 whereas the phases for the 531dW in IMF5 and IMF6 are opposite with each other (Fig.8b2).
329 Comparing those synthetic results with the results from the x-component of the 1962-1977 series as
330 listed in Table 1, the amplitudes of the 531dW in IMF5 (44.1 mas) and IMF6 (33.2 mas) of the real
331 data are almost equal to those of the synthetic results. The results as shown in Figs. 8(c-d) and 8(e-f)
332 have a similar nature to the results as shown in Fig.s 8(a-b). Namely, the input 531dW signal is in
333 fact demodulated into IMF5, whereas the 531dW signal caused by the frequency modulation of CW
334 is demodulated into IMF6.

335 The frequency modulation mechanism of CW is an open question. If we accept the modulation
336 mechanism of CW addressed above, the results obtained from the PM series after using EEMD can
337 be appropriately explained. However, the excitation sources of the 531dW in IMF5 still cannot be
338 confirmed. We do not intend to answer this question in this study, but we will try to confirm the
339 531dW in the independent gravity records in the following section to further confirm its presence.
340

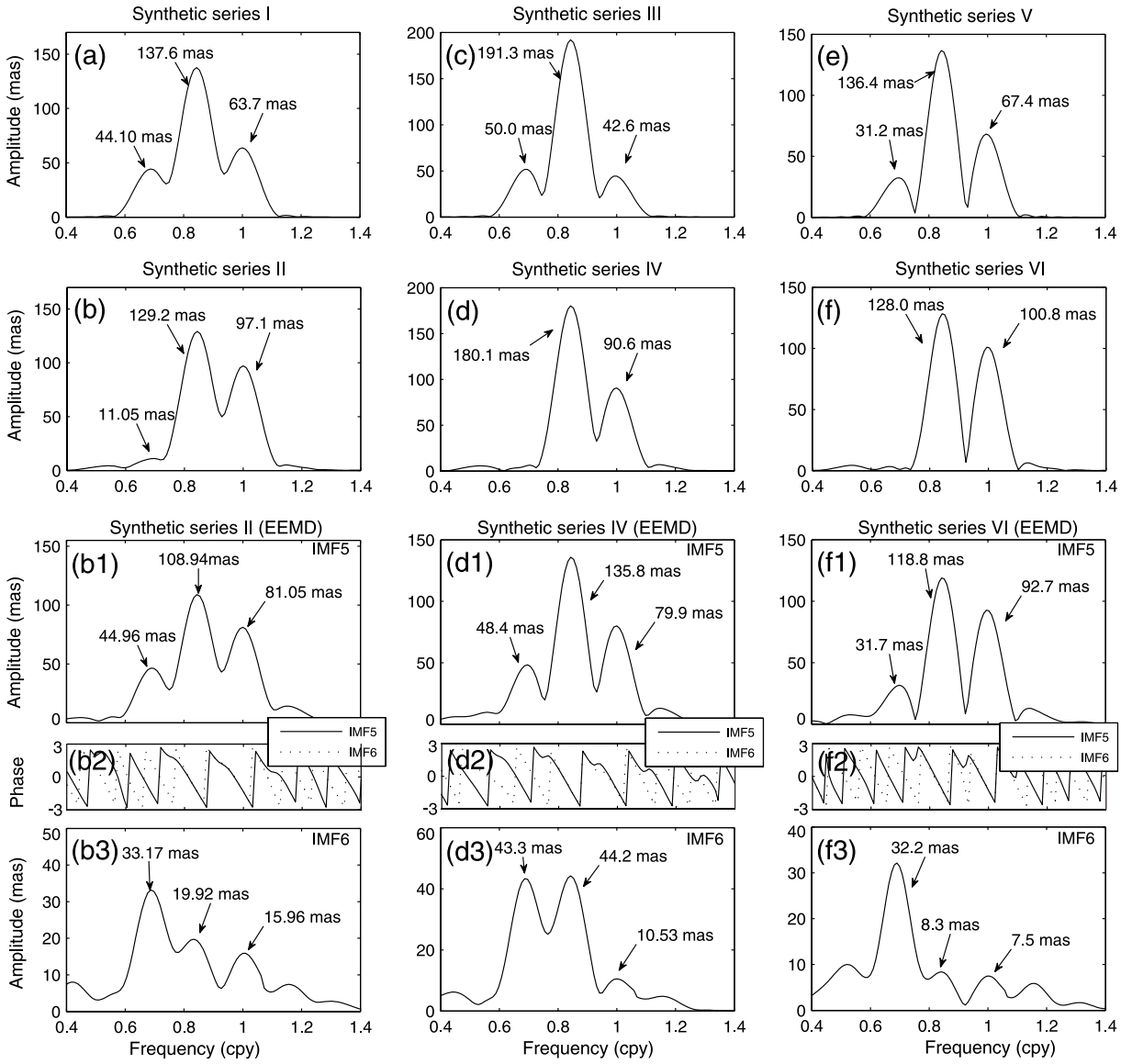

Figure 8. The amplitudes of the significant peaks (from left to right: 531dW, CW, AW) are marked by the arrows. The spectra of the synthetic series I (a) and II (b); and the spectra of the IMF5 and IMF6 of the synthetic series II after using EEMD (b1-b3). The spectra of the synthetic series III (c) and IV (d); and the spectra of the IMF5 and IMF6 of the synthetic series IV after using EEMD (d1-d3). The spectra of the synthetic series V (e) and VI (f); and the spectra of the IMF5 and IMF6 of the synthetic series VI after using EEMD (f1-f3).

3.3 Results from the SG records

If the 531dW can be excited by the atmospheric/oceanic angular momentum, or it is the normal mode of the Earth, it may be found in the gravity records. Hence, we choose the (superconducting gravimeter (SG) records from the Global Geodynamic Project (GGP) network to further confirm the existence of this signal. The GGP network has been operating about 25yr (from 1997), but the longest available continuous records (without very large gaps) are only about 16yr long, namely the records from the SG stations *Membach* (mb) (1995-2011) and *Medicina* (mc) (1998-2014). After removing the tidal effects (solid and ocean), the local atmospheric effect (without 531dW signal in it), and the pole tides, the spectra of the residual gravity records are shown in Fig. 9 (see the black curves). Two peaks around 531 dW can be found in Figs. 9a (for station mb) and 9b (for station mc). We have confirmed that the local atmospheric effect and the pole tides have no contributions to the 531dW. Since the pole tides have been removed, namely the CW, AW and the possible 531dW signals caused by the polar motion have been removed from the gravity records, the residual 531dW must be casued by some other sources. Here we further consider the hydrological loading (global) effect except the atmospheric loading (global) and non-tidal ocean loading effects (Petrov and Boy, 2004). The two latter effects are the same possible sources which excite the 531dW in PM series. However, Fig. 9 clearly shows those three effects cannot explain the residual 531dW, only the residual AW can be appropriately explained. This finding seems being not consistent with previous studies, but they can be explained. As Wahr (1983) and Chen et al. (2010) suggested, the 531dW can be excited by atmospheric/oceanic effects, and the excited signal by atmospheric or oceanic effect can be found in the PM series only after convoluting with the CW term. However, the 531dW signals excited by atmospheric and oceanic effect seem have different phases, hence the 531dW cannot be found in the PM series (Chen et al., 2010). If we accept this, the 531dW signal in gravity records

comes from two different sources: indirectly from polar motion which are affected by the atmospheric/oceanic effects, and directly from the atmospheric/oceanic effects. The excited 531dW from PM has been removed by taking away the pole tide effects. The excited 531dW directly from the atmospheric/oceanic effects has just the same nature as the excitation in the PM; if no convolution is processed with the CW, the 531dW signal cannot be found in the PM or gravity records. Hence, our findings are actually consistent with previous studies.

No matter how, our results clearly show the demodulation feature of EEMD is helpful for detecting the 531dW signal in the PM series, and we confirm that the amplitude and frequeny of the 531dW are varying with time.

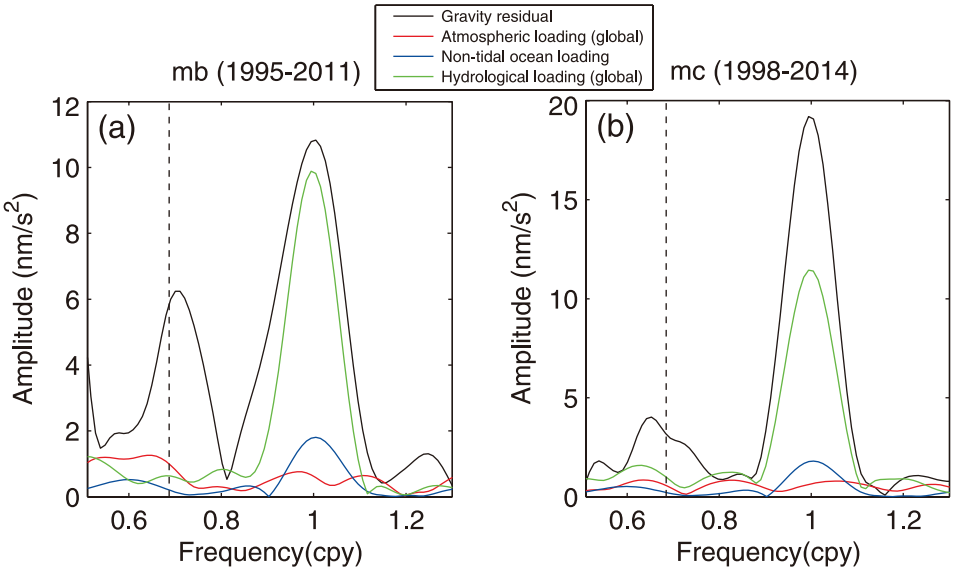

Figure 9. The Fourier spectra of the two residual SG records. (a) mb record; (b) mc record. The effects of the atmospheric loading (global), non-tidal ocean loading and the hydrological loading (global) are indicated by the red, blue and green curves, respectively.

4 Discussion and Conclusion

After applying EEMD to the 1962-2013 PM time series (EOP C04), a 531dW is clearly found

388 with a mean amplitude about 7mas (with much larger amplitudes in IMF5 and IMF6 series
389 respectively), but in the spectra without using EEMD, this signal cannot be found. The 531dW has
390 been found by previous studies in the 1962-1977 PM series with a lower SNR. To confirm previous
391 observations (Carter, 1981 and 1982) and further study this signal, we divide the whole PM series
392 into three sub-series, 1962-1977, 1978-1994 and 1995-2013 PM time series. Without using EEMD,
393 the results for the 1962-1977 PM series are consistent with previous studies, while the 531dW signal
394 disappears from the Fourier spectra of the 1978-1994 and 1995-2013 PM time series. However, after
395 applying EEMD to those three sub-series, the 531dW signals can be found in each sub-series with
396 different outstanding amplitudes (based on the spectra of the decomposed IMF5 and IMF6 series),
397 which (taking x-components as example) are respectively about 12.8 mas in 1962-1977, 4.0 mas in
398 1978-1994 and 3.4 mas in 1995-2013 (see Table 2), while the corresponding noise levels of the three
399 sub-series are about 9.5 mas, 8.8 mas and 5.4 mas recpectively. That is the reason why the 531dW
400 signal can only be directly found in the 1962-1977 PM series without using EEMD.

401 Although the frequency modulation mechanism of CW is an open question, we find that if the
402 modulation index M of CW equals 0.5, the results obtained from the PM series after using EEMD
403 can be appropriately explained. Furthermore, using synthetic tests we confirmed the demodulation
404 feature of EEMD which can help us find the 531dW signal in PM series, but this paper does not
405 attempt to explain the possible exctiation sources of the 531dW. Given that the 531dW signal can be
406 directly found in the SG records without using EEMD, it should be considered in the study of the
407 long period effects in some relevant geophycial datasets.

408 Though various previous studies have confirmed that the incomplete orthogonality of EEMD
409 hardly affects the analysis of many geophysical processes, it might still affect our PM time series

410 analysis process. Owing to the frequency and amplitude of the 531dW signal being time-varying
411 (Generally, they might be caused by the excited process and the background noise in different time
412 spanning), it becomes quite difficult to explore its excitations. It might be caused by the core
413 dynamics, or even by some random processes (e.g., Chao et al., 2014); but from the phase results of
414 the 531dW of King (2015), we may prefer to consider that the 531dW seems being excited by some
415 kind of unkown processes, which needs further investigations. Anyway, as a final conclusion, we
416 suggest that the 531dW signal exists in the nature, but left its mechanism open. With accumulation of
417 high-precise geodetic observation data, the long-period terms, such as 531dW, are to be further
418 studied, and this may help us better understand the Earth system.
419
420 **Acknowledgements**: We thank Jim Ray, Wei Chen and Benjamin Fong Chao for fruitful discussions
421 which improved the manuscript, and thank Christian Bizouard for helpful comments on an early
422 draft of this paper. We also thank Prof. M. King and two anonymous reviewers for their valuable
423 comments and suggestions, which significantly improved the manuscript. The atmospheric/
424 hydrological/ non-tidal ocean loading are provided by J.P. Boy (which can be downloaded from
425 http://loading.u-strasbg.fr/GGP/index.html). This study is supported by NSFC (grant No. 41174011),
426 National 973 Project China (grant No. 2013CB733305), NSFC (grant Nos. 41210006, 41429401,).
427
428 **Reference**
429 Carter, W. E.: Frequency modulation of the Chandlerian component of polar motion, J. Geophys.
430 Res., 86, 1653-1658, 1981.
431 Carter, W. E.: Refinements of the polar motion frequency modulation hypothesis, J. Geophys. Res.,

87, 7025-7028, 1982.

Chambers, D. P.: Evaluation of empirical mode decomposition for quantifying multi-decadal variations and acceleration in sea level records, Nonlin. Processes Geophys., 22, 157–166, 2015.

Chao, B. F.: Autoregressive harmonic analysis of the Earth's polar motion using homogeneous International Latitude Service data, J. Geophys. Res., 88, 10299-10307 (1983).

Chao, B. F., and Gilbert, F.: Autoregressive estimation of complex eigenfrequencies in low frequency seismic spectra, Geophys. J. Roy. Astron. Soc., 63, 641-657 (1980).

Chao, B. F., Chung, W. Y., Shih, Z. R. and Hsieh, Y. K.: Earth's rotation variations: a wavelet analysis, Terra Nova, 26, 260-264, 2014.

Chen, W., Shen, W. B. and Dong, X. W., Atmospheric Excitation of Polar Motion, Geo-spatial Information Science, 13(2), 130-136, 2010.

Chen, W., Shen, W. B., Han, J. and Li, J.: Free wobble of the triaxial Earth: theory and comparisons with International Earth Rotation Service (IERS) data, Surv. Geophys., 30, 39-49, 2009.

Chen, W., Ray, J., Li, J., Huang, C., and Shen, W.: Polar motion excitations for an Earth model with frequency-dependent responses: 1. A refined theory with insight into the Earth's rheology and core-mantle coupling, J. Geophys. Res., 118, 1–20, doi:10.1002/jgrb.50314, 2013.

Chen, W., Ray, J., Li, J., Shen, W., and Huang, C.: Polarmotion excitations for an Earth model with frequency-dependent responses: 2. Numerical tests of the meteorological excitations, J. Geophys. Res., 118, 1–13, doi:10.1002/jgrb.50313, 2013.

Ding, H., Chao, B.F.: Detecting harmonic signals in a noisy time-series: the z-domain Autoregressive (AR-z) spectrum, Geophys. J. Int., 201, 1287-1296, 2015.

453 Ding, H., Shen, W.B.: Determination of the complex frequencies for the normal modes below 1mHz
454 after the 2010 Maule and 2011 Tohoku earthquakes, Ann. Geophys., 56 (5),
455 doi:10.4401/ag-6400, 2013.

456 Franzke, C.: Multi-scale analysis of teleconnection indices: climate noise and nonlinear trend
457 analysis, Nonlin. Processes Geophys., 16, 65–76, 2009.

458 Gross, R. S., Fukumori, I. and Menemenlis, D.: Atmospheric and oceanic excitation of the Earth's
459 wobbles during 1980–2000, J. Geophys. Res., 108(B8), 2370, doi:10.1029/2002JB002143,
460 2003.

461 Höpfner, J.: Chandler and annual wobbles based on space-geodetic measurements, J. Geodyn., 36,
462 369-381, 2003.

463 Huang, N.E., Shen, Z., Long, S.R., Wu, M.C., Shih, H.H., Zheng, Q., Yen, N.C., Tung, C. C. and Liu,
464 H.H.: A review on Hilbert-Huang transform: Method and its applications to geophysical studies,
465 Rev. Geophys., 46, RG2006, doi: 10.1029/2007RG000228, 2008.

466 Huang, N. E., et al.: The empirical mode decomposition and the Hilbert spectrum for nonlinear and
467 non-stationary time series analysis, Proc. Roy. Soc. Lond., A454, 903-995, 1998.

468 Jackson, L. P. and Mound, J. E., Geomagnetic variation on decadal time scales: What can we learn
469 from Empirical Mode Decomposition? Geophy. Res. Lett., 37, L14307, doi:
470 10.1029/2010GL043455, 2010.

471 King, M., Interactive comment on "Search for the 531 day-period wobble signal in the polar motion
472 based on EEMD" by H. Ding and W. B. Shen, Nonlin. Processes Geophys. Discuss., 2, C163–
473 C168, 2015.

King, M. A. and Watson, C.S., Geodetic vertical velocities affected by recent rapid changes in polar motion, Geophys. J. Int., 199, 1161-1165, 2014.

Lee, T., and Ouarda, T. B. M. J.: Prediction of climate nonstationary oscillation processes with empirical mode decomposition, J. Geophys. Res., 116, D06107, doi: 10.1029/2010JD015142, 2011.

Liu, H. Y., Lin, Z. S., Qi, X. Z., Li, Y. X., Yu, M. T., Yang, H., and Shen, J.: Possible link between Holocene East Asian monsoon and solar activity obtained from the EMD method, Nonlin. Processes Geophys., 19, 421-430, 2012.

Morgan, P. J., King, R. W. and Shapiro, I. I.: Spectral analysis of variation of latitude derived from lunar laser ranging and satellite Doppler observations (abstract), Eos Trans., AGU, 63, 302, 1982.

Na, S., Cho, J., Baek, J., Kwak, Y., Yoo, S., Cho, S., Lim, H., Kwak, Y., Park, J. and Park, P.: 500-day period component in the Earth's polar motion (abstract). AGU Fall Meeting, San Francisco, California, USA, 2011/11, G53B-0910, 2011.

Okubo, S.: Is the Chandler period variable? Geophys. J. R. Astron. Soc., 71, 629-646, 1982.

Pan, C.: Linearization of the Liouville equation multiple splits of the Chandler frequency Markowitz wobbles and error analysis. International Journal of Geosciences, 3, 930-951, 2012.

Pee, M. C. and McMahon, T. A., Recent frequency component changes in interannual climate variability, Geophys. Res. Lett., 33, L16810, doi:10.1029/2006GL025670, 2006.

Petrov, L. and J.-P. Boy, Study of the atmospheric pressure loading signal in VLBI observations, J. Geophys. Res., 109, B03405, doi: 10.1029/2003JB002500, 2004.

Seitz, F. and Schmidt, M.: Atmospheric and oceanic contributions to Chandler wobble excitation determined by wavelet filtering, J. Geophys. Res., 110, B11406, doi:10.1029/2005JB003826, 2005.

Shen, W. B. and Ding, H.: Observation of spheroidal normal mode multiplets below 1 mHz using ensemble empirical mode decomposition, Geophys. J. Int., 196, 1631-1642, 2014.

Tary, J. B., Herrera, R. H., Han, J., and van der Baan, M., Spectral estimation—What is new? What is next?, Rev. Geophys., 52, 723-749, 2014.

Thomas, E. R., Dennis, P. F., Bracegirdle, T. J. and Franzke, C.: Ice core evidence for significant 100-year regional warming on the Antarctic Peninsula, Geophys. Res. Lett., 36, L20704, doi: 10.1029/2009GL040104, 2009.

Vicente, R. O. and Wilson, C. R., On the variability of the Chandler frequency, J. Geophys. Res., 102(B9), 20439-20446, 1997.

Wahr, J.: The effects of the atmosphere and oceans on the Earth's wobble and on the seasonal variations in the length of day, II. Results, Geophys. J. R. Astr. Soc., 74, 451-487, 1983.

Wu, Z. H. and Huang, N. E.: Ensemble empirical mode decomposition: a noise-assisted data analysis method, Adv. Adapt. Data. Anal., 1, 1-41, 2009.